PROCEEDINGS OF SCIENCE

The Real Time Analysis framework of the Cherenkov Telescope Array's Large-Sized Telescope

Sami Caroff,[a,*] **Pierre Aubert,**[a] **Enrique Garcia,**[a] **Gilles Maurin,**[a] **Vincent Pollet**[a] **and Thomas Vuillaume**[a] **on behalf of the CTA-LST Project**

[a] *Univ. Savoie Mont Blanc, CNRS, Laboratoire d'Annecy de Physique des Particules - IN2P3, 74000 Annecy, France*

E-mail: sami.caroff@lapp.in2p3.fr

The Large-Sized Telescopes (LSTs) of the Cherenkov Telescope Array Observatory (CTAO) will play a crucial role in the study of transient gamma-ray sources, such as gamma-ray bursts and flaring active galactic nuclei. The low energy threshold of LSTs makes them particularly well suited for the detection of these phenomena. The ability to detect and analyze gamma-ray transients in real-time is essential for quickly identifying and studying these rare and fleeting events. In this conference, we will present recent advances in the real-time analysis of data from the LST-1, the first prototype of LST located in the Canary island of La Palma. We will discuss in particular the development of new algorithms for event reconstruction and background rejection. These advances will enable rapid identification and follow-up observation of transient gamma-ray sources, making the LST-1 a powerful tool for the study of the dynamic universe. The implementation of this framework in the future Array Control and Data Acquisition System (ACADA) of CTAO will be discussed as well, based on the experience with LST.

38th International Cosmic Ray Conference (ICRC2023)
26 July - 3 August, 2023
Nagoya, Japan

*Speaker

PoS(ICRC2023)616

1. Introduction

Gamma-ray astronomy aims to study the cosmic particle accelerators of the universe, through the analysis of their high-energy electromagnetic emissions. It covers various types of sources, from Galactic ones such as supernovae remnants and pulsar wind nebulae to extragalactic ones like active galactic nuclei. Recently, the first detections of the afterglow radiations from gamma-ray bursts [1–3] were achieved at very high energies (VHE, $E > 100$ GeV), opening a new research area around transient phenomena. Moreover, recent observations of the electromagnetic counterpart of gravitational wave emitters have motivated a fast development of the field.

The Cherenkov Telescope Array Observatory (CTAO) represents the next generation of ground-based observatories. In October 2018, the first prototype of the Large-Sized Telescope, called LST-1, was installed and inaugurated at the Roque de los Muchachos Observatory (ORM). It has been actively collecting data since November 2019. The LST-1 boasts a 23-meters diameter reflector dish, a lightweight mechanical structure, and a rapid repositioning system. Its primary purpose is to detect low-energy gamma rays, above approximately 20 GeV, and to enable swift follow-up observations of transient events. Efficiently monitoring alerts and observing transient events is only possible with a robust and fast (real-time) analysis system, which processes data immediately after they are collected during observations and provides timely feedback to operators to initiate appropriate decisions and generate alerts. The analysis process can be divided into two sequential stages: first, the reconstruction, characterization, and selection of gamma rays from the recorded images, and second, the search for sources within the telescope's field of view.

This proceeding only covers the first part which is the real-time analysis (RTA) of the LST-1, prototype of the CTAO online-reconstruction. Section 2 describes the global architecture and the technical options adopted while section 3 exposes the performance and results obtained on Markarian 421 data.

2. Data Analysis

The initial stage of the analysis process, known as reconstruction, focuses on processing the uncalibrated raw data (R0) to derive the parameters of each recorded event (DL3-data). These parameters include the energy, direction, and a gamma-ray like classification score (called gammaness). The LST-1 telescope R0 data consists of a sequences of 40 images, each containing 1855 pixels, for every recorded event. In its nominal mode, the telescope operates at a rate of ∼10 kHz, generating a data flow of ∼3 GB/s of the raw data but the rate can go up to 15 kHz in case of extreme astrophysical events. Looking ahead to the future CTA observatory, the expected data flow will be approximately 17 GB/s for the northern site and 27 GB/s for the southern site.

The historical Hillas method [4] serves as the reference reconstruction approach, renowned for its simplicity and robustness. Its modern version comprises three consecutive stages, implemented in three corresponding software blocks:

- The **R0->DL1** stage includes data calibration, images aggregation and cleaning for each event. It also encompasses the extraction of Hillas and timing parameters (as defined in [5]). This stage significantly reduces the data volume from several GB/s to less than 150 MB/s.

Most of the output data consists of the final calibrated images used for monitoring the data acquisition (DAQ), while the Hillas parameters correpond to only a few MB/s.

- The **DL1->DL2** stage focuses on evaluating the energy, direction, and gammaness. The input and output data sizes are approximately the same, amounting to a few MB/s.
- **DL2->DL3** stage corresponds to the selection of gamma-like events, further reducing the data flow to a few kB/s.

2.1 Software Architecture

To ensure seamless data acquisition, the RTA is performed on dedicated servers, with communication between the DAQ system and the analysis servers established through the network. At least two servers are required to receive data from the LST-1. R0 data is streamed in the Protocol Buffer format[1] handled by ZeroMQ[2], an open-source universal messaging library.

The Slurm[3] workload manager plays a vital role in resources and processes management. This open-source, fault-tolerant, and highly scalable cluster management and job scheduling system is specifically designed for both large and small Linux clusters.

On each server, four processes of R0->DL1, each with two threads, continuously run to process the data stream. Each thread handles an approximate event rate of 1.25 kHz, resulting in a total processing capacity of 10 kHz under nominal operation. Evaluation of the events produced by Car flash[4] indicates that the maximum rate of 15 kHz (1.875 kHz) provided by the LST-1 is supported by the analysis servers. A short buffer of 100 events, equivalent to 80 ms of data, is used.

Following the R0->DL1 computation, HDF5[5][6] files containing 20 000 DL1 events are generated. For each new file, the DL1->DL2->DL3 chain is immediately executed using the capabilities of the Slurm manager.

2.2 Optimization of data processing

The RTA includes several stages: image calibration, selection, integration, cleaning, and extraction of Hillas parameters. The data reduction and processing steps are computationally demanding, therefore, the C++ programming language was chosen for its fast execution and optimization capabilities.

The calibration step consists in converting electronic charge into the corresponding number of photoelectrons detected by each camera pixel by subtracting a baseline (pedestal) and applying a conversion factor (gain) . The calibration algorithm selects the appropriate gains and pedestals obtained with calibration runs. The compiler automatically vectorizes this algorithm for improved performance.

Pixel-wise charge integration involves summing the calibrated signals for each pixel using a specific time window. The compiler can optimize this process by effectively vectorizing the integration calculations.

[1] https://developers.google.com/protocol-buffers/docs/overview
[2] https://zeromq.org
[3] https://slurm.schedmd.com/documentation.html
[4] Car flash events are induced by the illuminations of car passing by the road near the telescope.
[5] https://support.hdfgroup.org/HDF5/
[6] https://gitlab.in2p3.fr/CTA-LAPP/PHOENIX_LIBS/PhoenixHDF5/

Image cleaning is performed to select relevant pixels and remove those which triggered due to background noise. A two-thresholds algorithm (thresholding on pixel and pixel neighbours charge) is applied using a temporary matrix to ensure efficient memory access for neighboring pixels. Computation is performed instead of branching, which improves computational time by enabling vectorization.

Hillas and timing parameters are computed to characterize the shape of the cleaned images and extract relevant information. High-level intrinsic functions[7] are used to optimize reduction operations and barycenter computations, resulting in faster execution compared to automatic optimization methods.

Overall, these optimization techniques aim to reduce the computation time and enhance the performance of the data processing pipeline.

2.3 High level parameters computation and DL3 production

The computation of the high-level parameters is not a bottleneck in terms of computing time, therefore the offline analysis chain of the LST-1 is used in order to simplify the maintainability of the software. This offline analysis chain is described in [5] and only a brief description will be provided in this proceeding. This analysis pipeline is working with a different DL1 format (hereafter called DL1-lstchain) than the CTAO standard one. Thus to use it a conversion step is required in the pipeline.

The high-level parameters, disp, energy, and gammaness are obtained using random forests trained on Monte Carlo simulations of gamma-ray events generated with a zenith angle of 20°. Similar results with respect to those of the offline trained random forest [5] are obtained: time gradient is the most important feature for disp reconstruction, followed by psi, and length Hillas parameters, while the length is the most important feature for energy. For gammaness classification, features ranking is more equally distributed.

The last part of the analysis consists of a gammaness selection and a conversion to a FITS format compliant with gammapy, a high-level analysis software [6].

3. Performance

3.1 Computing time

As explained in section 2, the software should support an event rate up to 15 kHz. Trigger rate peaks are exploited to test this requirement. An example is shown in Figure 1: it can be observed that the DL1 reconstruction was not affected by an event rate peak of 14 kHz.

The typical time for the production of the different analysis steps, is estimated using an observation run with an average rate of $\sim$ 8 kHz:

- R0->DL1 : 30 s. Taking that the effective rate per thread before cleaning is 1 kHz, and that 20k events need to be accumulated to create a DL1 file, the analysis time can be approximated as 10 seconds while the 20 remaining seconds are spend to accumulate events. The offline chain for the DL1 production is running at 0.03 s/event while the RTA achieve a computing speed of 0.5 ms/event.

[7] https://gitlab.in2p3.fr/CTA-LAPP/PHOENIX_LIBS/IntrinsicsGenerator/

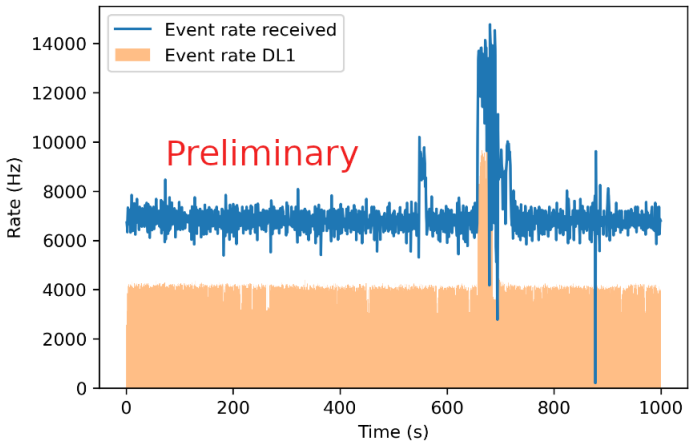

Figure 1: Rate of event received by the R0->DL1 process compared to the rate of events in DL1. The observed difference in normalisation is due to the cleaning step which rejects some of the events.

- DL1->DL1 lstchain : 12 s are used for this step, which will disappear when lstchain data format aligns with CTAO's in future releases.
- DL1 lstchain->DL2->DL3 : 14 + 10 s.

In total, 66 seconds are needed to produce a DL3 from 20k R0 events. It is important to note that this time scales linearly with the number of events per file.

3.2 Reconstruction

The reconstruction performance is tested using real time data obtained from observations of Markarian 421. They consist of 14 observations selected according to the weather on site, variability of event rate at the DL3 level and zenith angle lower than 30°, amounting to 4.2 hours of observations. These data were reconstructed with both the RTA and the lstchain pipeline. We used the same Monte Carlo simulation to train the random forest used by both pipelines.

The first step consists to optimizing the gammaness threshold. This was done separately on the two chains, by performing a full multiple OFF analysis of a single run of the dataset that is then removed for the rest of the analysis. The size of the ON region is set to 0.2° and the exclusion region defined as 0.35°. The same setup will be used in all this proceeding. A maximum significance of 15.3σ with a gammaness threshold of 0.75 for the RTA, and 31.2σ with 0.7 for the offline analysis are found. The effective area, energy bias and resolution, computed using the gamma Monte Carlo simulations, are displayed in figure 2. The energy resolution and bias are similar between the two analysis chains above 400 GeV, and a degradation is observed at the lowest energy for the RTA when compared to the lstchain reconstruction. The relative value of the effective area is linked to the leakage of events up to 0.2° and is thus related to a worse angular resolution for the RTA analysis chain.

A multiple off analysis is performed on the whole dataset, and the resulting theta square plot is presented in figure 3. A significance of 43.3σ for the RTA and 83.1σ for the offline analysis are found.

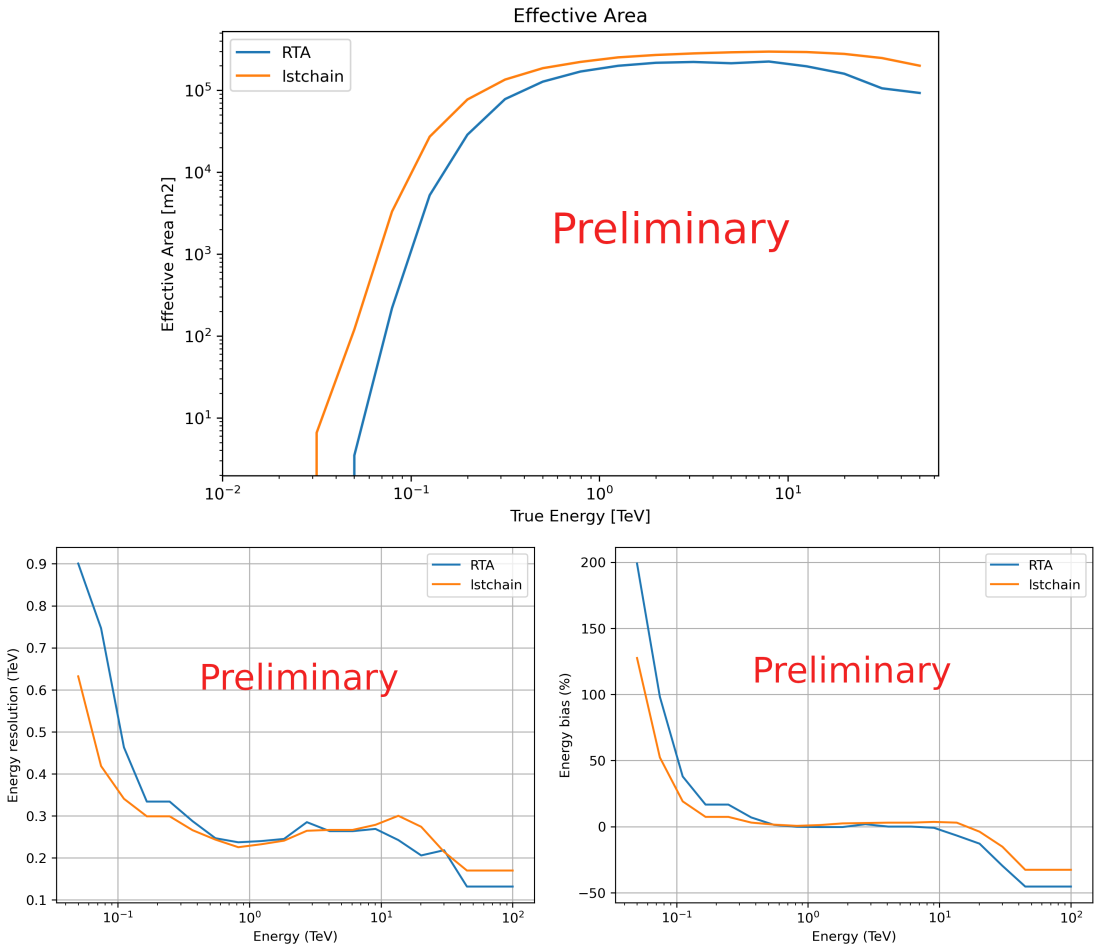

Figure 2: Effective area, energy resolution and bias in function of energy, computed in the gamma Monte Carlo.

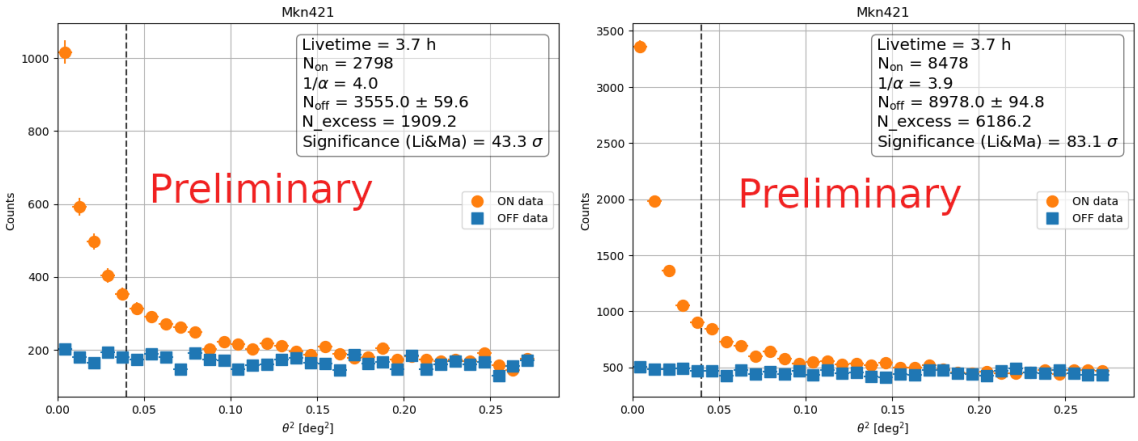

Figure 3: Theta square plot of Markarian 421 data compared between the RTA (left) and the lstchain (right).

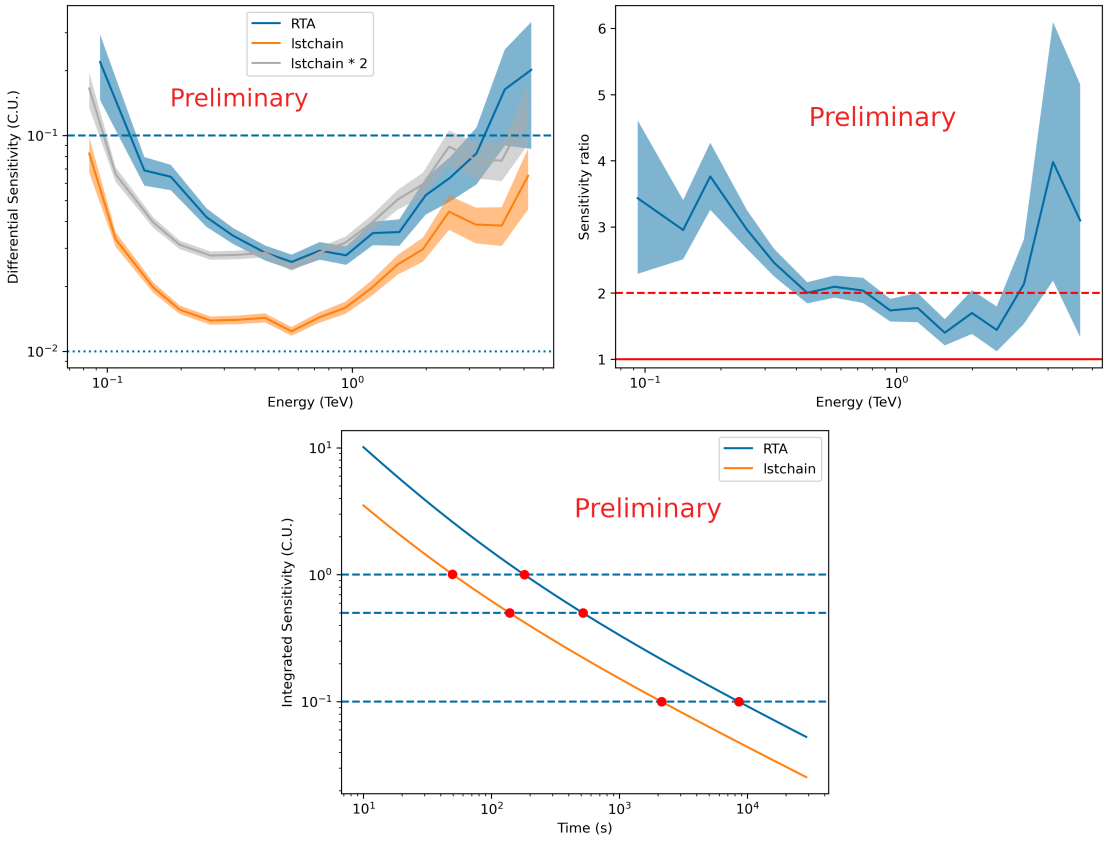

Figure 4: Top left : Differential Sensitivity for 50 hours of the RTA compared with lstchain as a function of true energy. Top right : Sensitivity ratio between the RTA and lstchain as a function of true energy. Down : Integral Sensitivity, from 20 GeV to 10 TeV, of the RTA compared to a typical flux of 1, 0.5 and 0.1 Crab, as a function of observation time. The time to detect the typical fluxes with the RTA is respectively 177, 517 and 8580 seconds. For the offline analysis, we have respectively 50, 139 and 2140 seconds.

The spectra of the source is reconstructed with the lstchain pipeline, which has been validated for this purpose, and used in order to derive the sensitivity of both chains. Differential sensitivity is defined as the minimal flux needed to have a 5σ detection in 50 hours of observations. The results are presented in figure 4. The sensitivity of the RTA pipeline is roughly two times worse than the lstchain one above 0.4 TeV, while at lower energies it worsens.

Besides the differential sensitivity, an important RTA use case is to detect a source in a time period shorter than a run (20 minutes). To explore this possibility, we provide the integral sensitivity versus time, supposing a Crab nebula like spectra, based on the results obtained on the test sample. This is presented in the figure 4. The RTA is able to detect an integrated flux of 0.3 Crab units in a single run.

4. Conclusions and outlook

In this proceeding, we presented the software architecture and performance of the RTA of the LST-1. Production of DL3 files from 20k events takes 66 seconds, and a flux equivalent to the one

of the Crab Nebula above 20 GeV can be detected in 177 seconds. The differential sensitivity of the RTA is two times worse than the offline analysis chain above 400 GeV.

The differences with lstchain is mainly due to two main factors. The first one is the timing parameters computation, particularly useful for the angular resolution, which is performed using a simple linear regression in the RTA for time computing reasons. Moreover, the performed calibration is simplified to gain and pedestal calibration while a full calibration chain imply as well the so-called DRS4 calibration [8].

The RTA will be provided to the Array Control and Data Acquisition System (ACADA) [9] of CTAO for its first release, with no differences with the version presented in this proceeding apart the input calibrated stream. The CTAO speed requirement of 1000 events/CPU/Tel is already fulfilled. The adaptation of this software to the full array will require modifications mostly at the DL1 level, to merge triggered events, and to DL2 production to take into account the stereoscopic reconstruction. Nevertheless, the scalability and modularity of this software was designed to fulfill this goal in the coming years for the construction of the LST2-4 telescopes and the next releases of ACADA.

Acknowledgements

The aknowledgements for CTAO and LST can be found here and here.

References

[1] Abdalla, H., Adam, R., Aharonian, F. et al. A very-high-energy component deep in the γ-ray burst afterglow. Nature 575, 464–467 (2019).

[2] MAGIC Collaboration., Veres, P., Bhat, P.N. et al. Observation of inverse Compton emission from a long γ-ray burst. Nature 575, 459–463 (2019).

[3] H.E.S.S. Collaboration, Revealing x-ray and gamma ray temporal and spectral similarities in the GRB 190829A afterglow. Science 372,1081-1085(2021).

[4] Hillas, A.M., Cerenkov light images of EAS produced by primary gamma,Proc. of 19nd I.C.R.C. (La Jolla), 3 445 (1985)

[5] Observations of the Crab Nebula and Pulsar with the Large-Sized Telescope prototype of the Cherenkov Telescope Array - eprint arXiv:2306.12960

[6] Gammapy - A prototype for the CTA science tools Proc. 35th ICRC, Busan, South Korea, PoS(ICRC2017)766

[7] Rubén López-Coto, et al.. lstchain: An Analysis Pipeline for LST-1, the First Prototype Large-Sized Telescope of CTA. 30th ADASS, Nov 2020, Granada, Spain. pp.357.

[8] Yukiho Kobayashi, et al.. Camera Calibration of the CTA-LST prototype. 37th ICRC, Jul 2021, Berlin, Germany. pp.720

[9] Igor Oya, et al.. The Array Control and Data Acquisition System of the Cherenkov Telescope Array. 17th ICALEPCS, Oct 2019, New York, United States.

Full Author list of the CTA-LST Project:

K. Abe[1], S. Abe[2], A. Aguasca-Cabot[3], I. Agudo[4], N. Alvarez Crespo[5], L. A. Antonelli[6], C. Aramo[7], A. Arbet-Engels[8], C. Arcaro[9], M. Artero[10], K. Asano[2], P. Aubert[11], A. Baktash[12], A. Bamba[13], A. Baquero Larriva[5,14], L. Baroncelli[15], U. Barres de Almeida[16], J. A. Barrio[5], I. Batkovic[9], J. Baxter[2], J. Becerra González[17], E. Bernardini[9], M. I. Bernardos[4], J. Bernete Medrano[18], A. Berti[8], P. Bhattacharjee[11], N. Biederbeck[19], C. Bigongiari[6], E. Bissaldi[20], O. Blanch[10], G. Bonnoli[21], P. Bordas[3], A. Bulgarelli[15], I. Burelli[22], L. Burmistrov[23], M. Buscemi[24], M. Cardillo[25], S. Caroff[11], A. Carosi[6], M. S. Carrasco[26], F. Cassol[26], D. Cauz[22], D. Cerasole[27], G. Ceribella[8], Y. Chai[8], K. Cheng[2], A. Chiavassa[28], M. Chikawa[2], L. Chytka[29], A. Cifuentes[18], J. L. Contreras[5], J. Cortina[18], H. Costantini[26], M. Dalchenko[23], F. Dazzi[6], A. De Angelis[9], M. de Bony de Lavergne[11], B. De Lotto[22], M. De Lucia[7], R. de Menezes[28], L. Del Peral[30], G. Deleglise[11], C. Delgado[18], J. Delgado Mengual[31], D. della Volpe[23], M. Dellaiera[11], A. Di Piano[15], F. Di Pierro[28], A. Di Pilato[23], R. Di Tria[27], L. Di Venere[27], C. Díaz[18], R. M. Dominik[19], D. Dominis Prester[32], A. Donini[6], D. Dorner[33], M. Doro[9], L. Eisenberger[33], D. Elsässer[19], G. Emery[26], J. Escudero[4], V. Fallah Ramazani[34], G. Ferrara[24], F. Ferrarotto[35], A. Fiasson[11,36], L. Foffano[25], L. Freixas Coromina[18], S. Fröse[19], S. Fukami[2], Y. Fukazawa[37], E. Garcia[11], R. Garcia López[17], C. Gasbarra[38], D. Gasparrini[38], D. Geyer[19], J. Giesbrecht Paiva[16], N. Giglietto[20], F. Giordano[27], P. Gliwny[39], N. Godinovic[40], R. Grau[10], J. Green[8], D. Green[8], S. Gunji[41], P. Günther[33], J. Hackfeld[34], D. Hadasch[2], A. Hahn[8], K. Hashiyama[2], T. Hassan[18], K. Hayashi[2], L. Heckmann[8], M. Heller[23], J. Herrera Llorente[17], K. Hirotani[2], D. Hoffmann[26], D. Horns[12], J. Houles[26], M. Hrabovsky[29], D. Hrupec[42], D. Hui[2], M. Hütten[2], M. Iarlori[43], R. Imazawa[37], T. Inada[2], Y. Inome[2], K. Ioka[44], M. Iori[35], K. Ishio[39], I. Jimenez Martinez[18], J. Jurysek[45], M. Kagaya[2], V. Karas[46], H. Katagiri[47], J. Kataoka[48], D. Kerszberg[10], Y. Kobayashi[2], K. Kohri[49], A. Kong[2], H. Kubo[2], J. Kushida[1], M. Lainez[5], G. Lamanna[11], A. Lamastra[6], T. Le Flour[11], M. Linhoff[19], F. Longo[50], R. López-Coto[4], A. López-Oramas[17], S. Loporchio[27], A. Lorini[51], J. Lozano Bahilo[30], P. L. Luque-Escamilla[52], P. Majumdar[53,2], M. Makariev[54], D. Mandat[45], M. Manganaro[32], G. Manicò[24], K. Mannheim[33], M. Mariotti[9], P. Marquez[10], G. Marsella[24,55], J. Marti[52], O. Martinez[56], G. Martínez[18], M. Martínez[10], A. Mas-Aguilar[5], G. Maurin[11], D. Mazin[2,8], E. Mestre Guillen[52], S. Micanovic[32], D. Miceli[9], T. Miener[5], J. M. Miranda[56], R. Mirzoyan[8], T. Mizuno[57], M. Molero Gonzalez[17], E. Molina[3], T. Montaruli[23], I. Monteiro[11], A. Moralejo[10], D. Morcuende[4], A. Morselli[38], V. Moya[5], H. Muraishi[58], K. Murase[2], S. Nagataki[59], T. Nakamori[41], A. Neronov[60], L. Nickel[19], M. Nievas Rosillo[17], K. Nishijima[1], K. Noda[2], D. Nosek[61], S. Nozaki[8], M. Ohishi[2], Y. Ohtani[2], T. Oka[62], A. Okumura[63,64], R. Orito[65], J. Otero-Santos[17], M. Palatiello[22], D. Paneque[8], F. R. Pantaleo[20], R. Paoletti[51], J. M. Paredes[3], M. Pech[45,29], M. Pecimotika[32], M. Peresano[28], F. Pfeiffle[33], E. Pietropaolo[66], G. Pirola[8], C. Plard[11], F. Podobnik[51], V. Poireau[11], V. Pollet[11], M. Polo[18], E. Pons[11], E. Prandini[9], J. Prast[11], G. Principe[50], C. Priyadarshi[10], M. Prouza[45], R. Rando[9], W. Rhode[19], M. Ribó[3], C. Righi[21], V. Rizi[66], G. Rodriguez Fernandez[38], M. D. Rodríguez Frías[30], T. Saito[2], S. Sakurai[2], D. A. Sanchez[11], T. Šarić[40], Y. Sato[67], F. G. Saturni[6], V. Savchenko[60], B. Schleicher[33], F. Schmuckermaier[8], J. L. Schubert[19], F. Schussler[68], T. Schweizer[8], M. Seglar Arroyo[11], T. Siegert[33], R. Silvia[27], J. Sitarek[39], V. Sliusar[69], A. Spolon[9], J. Strišković[42], M. Strzys[2], Y. Suda[37], H. Tajima[63], M. Takahashi[63], H. Takahashi[37], J. Takata[2], R. Takeishi[2], P. H. T. Tam[2], S. J. Tanaka[67], D. Tateishi[70], P. Temnikov[54], Y. Terada[70], K. Terauchi[62], T. Terzic[32], M. Teshima[8,2], M. Tluczykont[12], F. Tokanai[41], D. F. Torres[71], P. Travnicek[45], S. Truzzi[51], A. Tutone[6], M. Vacula[29], P. Vallania[28], J. van Scherpenberg[8], M. Vázquez Acosta[17], I. Viale[9], A. Vigliano[22], C. F. Vigorito[28,72], V. Vitale[38], G. Voutsinas[23], I. Vovk[2], T. Vuillaume[11], R. Walter[69], Z. Wei[71], M. Will[8], T. Yamamoto[73], R. Yamazaki[67], T. Yoshida[47], T. Yoshikoshi[2], N. Zywucka[39], [1]Department of Physics, Tokai University. [2]Institute for Cosmic Ray Research, University of Tokyo. [3]Departament de Física Quàntica i Astrofísica, Institut de Ciències del Cosmos, Universitat de Barcelona, IEEC-UB. [4]Instituto de Astrofísica de Andalucía-CSIC. [5]EMFTEL department and IPARCOS, Universidad Complutense de Madrid. [6]INAF - Osservatorio Astronomico di Roma. [7]INFN Sezione di Napoli. [8]Max-Planck-Institut für Physik. [9]INFN Sezione di Padova and Università degli Studi di Padova. [10]Institut de Fisica d'Altes Energies (IFAE), The Barcelona Institute of Science and Technology. [11]LAPP, Univ. Grenoble Alpes, Univ. Savoie Mont Blanc, CNRS-IN2P3, Annecy. [12]Universität Hamburg, Institut für Experimentalphysik. [13]Graduate School of Science, University of Tokyo. [14]Universidad del Azuay. [15]INAF - Osservatorio di Astrofisica e Scienza dello spazio di Bologna. [16]Centro Brasileiro de Pesquisas Físicas. [17]Instituto de Astrofísica de Canarias and Departamento de Astrofísica, Universidad de La Laguna. [18]CIEMAT. [19]Department of Physics, TU Dortmund University. [20]INFN Sezione di Bari and Politecnico di Bari. [21]INAF - Osservatorio Astronomico di Brera. [22]INFN Sezione di Trieste and Università degli Studi di Udine. [23]University of Geneva - Département de physique nucléaire et corpusculaire. [24]INFN Sezione di Catania. [25]INAF - Istituto di Astrofisica e Planetologia Spaziali (IAPS). [26]Aix Marseille Univ, CNRS/IN2P3, CPPM. [27]INFN Sezione di Bari and Università di Bari. [28]INFN Sezione di Torino. [29]Palacky University Olomouc, Faculty of Science. [30]University of Alcalá UAH. [31]Port d'Informació Científica. [32]University of Rijeka, Department of Physics. [33]Institute for Theoretical Physics and Astrophysics, Universität Würzburg. [34]Institut für Theoretische Physik, Lehrstuhl IV: Plasma-Astroteilchenphysik, Ruhr-Universität Bochum. [35]INFN Sezione di Roma La Sapienza. [36]ILANCE, CNRS . [37]Physics Program, Graduate School of Advanced Science and Engineering, Hiroshima University. [38]INFN Sezione di Roma Tor Vergata. [39]Faculty of Physics and Applied Informatics, University of Lodz. [40]University of Split, FESB. [41]Department of Physics, Yamagata University. [42]Josip Juraj Strossmayer University of Osijek, Department of Physics. [43]INFN Dipartimento di Scienze Fisiche e Chimiche - Università degli Studi dell'Aquila and Gran Sasso Science Institute. [44]Yukawa Institute for Theoretical Physics, Kyoto University. [45]FZU - Institute of Physics of the Czech Academy of Sciences. [46]Astronomical Institute of the Czech Academy of Sciences. [47]Faculty of Science, Ibaraki University. [48]Faculty of Science and Engineering, Waseda University. [49]Institute of Particle and Nuclear Studies, KEK (High Energy Accelerator Research Organization). [50]INFN Sezione di Trieste and Università degli Studi di Trieste. [51]INFN and Università degli Studi di Siena, Dipartimento di Scienze Fisiche, della Terra e dell'Ambiente (DSFTA). [52]Escuela Politécnica Superior de Jaén, Universidad de Jaén. [53]Saha Institute of Nuclear Physics. [54]Institute for Nuclear Research and Nuclear Energy, Bulgarian Academy of Sciences. [55]Dipartimento di Fisica e Chimica 'E. Segrè' Università degli Studi di Palermo. [56]Grupo de Electronica, Universidad Complutense de Madrid. [57]Hiroshima Astrophysical Science Center, Hiroshima University. [58]School of Allied Health Sciences, Kitasato University. [59]RIKEN, Institute of Physical and Chemical Research. [60]Laboratory for High Energy Physics, École Polytechnique Fédérale. [61]Charles University, Institute of Particle and Nuclear Physics. [62]Division of Physics and Astronomy, Graduate School of Science, Kyoto University. [63]Institute for Space-Earth Environmental Research, Nagoya University. [64]Kobayashi-Maskawa Institute (KMI) for the Origin of Particles and the Universe, Nagoya University. [65]Graduate School of Technology, Industrial and Social Sciences, Tokushima University. [66]INFN Dipartimento di Scienze Fisiche e Chimiche - Università degli Studi dell'Aquila and Gran Sasso Science Institute. [67]Department of Physical Sciences, Aoyama Gakuin University. [68]IRFU, CEA, Université Paris-Saclay. [69]Department of Astronomy, University of Geneva. [70]Graduate School of Science and Engineering, Saitama University. [71]Institute of Space Sciences (ICE-CSIC), and Institut d'Estudis Espacials de Catalunya (IEEC), and Institució Catalana de Recerca I Estudis Avançats (ICREA). [72]Dipartimento di Fisica - Universitá degli Studi di Torino. [73]Department of Physics, Konan University.

PoS(ICRC2023)616